Experimental Investigation of Common Mode Current Generation in a Novel Dual Active Bridge Converter ZVS Modulation Pattern

Kubilay Sahin, Jean-Luc Schanen, Sébastien Mariéthoz, Yann Cuenin

Experimental Investigation of Common Mode Current Generation in a Novel Dual Active Bridge Converter ZVS Modulation Pattern

Kubilay Sahin
Power Electronics Laboratory
Bern University of Applied Sciences
Biel/Bienne, Switzerland
kubilay.sahin@bfh.ch

Jean-Luc Schanen
G2Elab
Grenoble Alpes University
Grenoble, France
jean-luc.schanen@g2elab.grenoble-inp.fr

Sébastien Mariéthoz
Power Electronics Laboratory
Bern University of Applied Sciences
Biel/Bienne, Switzerland
sebastien.mariethoz@bfh.ch

Yann Cuenin
Studer Innotec SA
Sion, Switzerland
yann.cuenin@studer-innotec.com

***Abstract*—This paper deals with the experimental comparison of two modulation patterns for the Dual Active Bridge Converter (DAB) regarding common mode current generation. One of them is the well known Triangular modulation which leads to minimal conduction losses and switches with ZVS and ZCS. The other one is a new modulation pattern proposed by our research group, which makes it possible to switch in a larger operating range with ZVS without having to adjust the switching frequency or the magnetizing inductance of the transformer, which was up to now not possible. The measurement results of the created common mode current were evaluated in the time domain and in the frequency domain for each modulation pattern and an attempt was made to graphically reproduce the switch positions of the two modulation patterns using electrical circuit diagrams in order to conclude the generation of the common mode current. It was discovered experimentally that the proposed novel modulation pattern generates less common mode current for a wide frequency range, although it is switched more often.**

***Index Terms*—Common mode current, DAB, Modulation pattern, ZVS,**

I. Introduction

The losses of the DAB [1] may be reduced by operating with ZVS [2]. Up to now, full coverage of the entire operating range with ZVS was only possible by changing the switching frequency [3] or adjusting the magnetizing inductance of the transformer [4]. A set of new modulation patterns which break this limitation is proposed by our research group. One is the DAB ZVS Triangular Small/Medium (S/M), which could be used for small to medium power transmissions. To enlarge the ZVS region, additional voltage pulses are used. It is interesting to know what influence these additional voltage pulses have on the common mode current generation. Therefore, a set-up was built and the new modulation pattern DAB ZVS Triangular S/M was experimentally compared with the conventional Triangular modulation [5] leading to minimal conduction losses and switching at zero voltage and zero current, which is further titled DAB ZVS ZCS Triangular.

II. Experimental common mode current evaluation

A. Set-up and its configuration

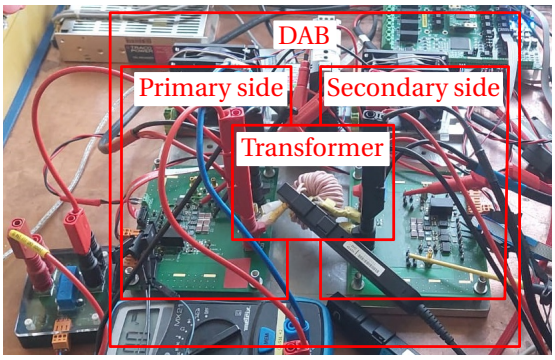

Fig. 1: DAB photo

On Figure 3 the DAB experimental set-up electric circuit diagram for the common mode current measurement is visible. The Fourline-V-LISN Type NNB-4/63TL [6] was used in order to create a well-defined impedance [7]. In the experiment the quantities u_A, u_B, i_L and i_{cm} were measured for the evaluation of the common mode current using the current probe Tektronix P6021 [8] with Tektronix TCPA300 [9] amplifier and the high voltage probe Tektronix THDP0200 [10]. The DAB was realized with two full bridge PCBs using EPC2302 eGaN FETs [11]. A high-frequency transformer with an N87 core, 16 primary and secondary windings and a leakage inductance of 3 µH was developed for the isolation. The operating point at which the two modulation patterns DAB ZVS ZCS Triangular and DAB ZVS Triangular S/M were compared was set to $fsw = 100\,\text{kHz}$, $U_{A_{dc}} = 60\,\text{V}$, $U_{B_{dc}} = 48\,\text{V}$ and $I_{B_{dc}} = 2\,\text{A}$. The converter was designed for

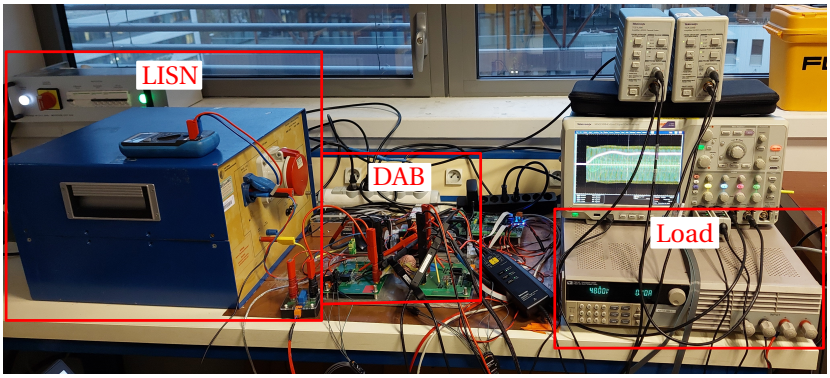

Fig. 2: DAB experimental set-up photo

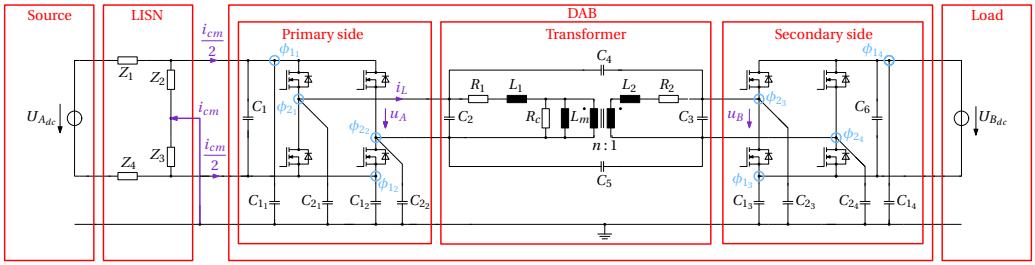

Fig. 3: DAB experimental set up electric circuit diagram

max. 600 W. A photo of the DAB is visible on Figure 1 and of the set-up on Figure 2.

B. DAB ZVS ZCS Triangular modulation pattern common mode current evaluation in the time domain

Transient	Description
1	By switching on S_1 and S_5, the potentials ϕ_{2_1} and ϕ_{2_3} increase with a positive and large $\frac{\Delta v}{\Delta t}$ and lead to a positive common mode current Figure 4.
2	By switching on S_3, the potential ϕ_{2_2} increase with a positive and large $\frac{\Delta v}{\Delta t}$ and lead to a positive common mode current Figure 5.
3	By opening S_5 and S_8, the transformer current i_L will naturally drop to zero. Conducting the eGaN FETs in the reverse direction results in a negative voltage u_5 and u_8. As the voltages u_5 and u_8 only decrease slightly and not with a strong slope, no common mode current is generated Figure 6.

TABLE I: DAB ZVS ZCS Triangular modulation pattern summary of common mode current generation

Figure 7 shows the measurement results of the DAB ZVS ZCS Triangular modulation pattern. The transients that generate the common mode current are marked as red shaded areas. The description of the respective transients can be seen in Table I. Figure 4 to Figure 6 also graphically show the switch states that generate the common mode current. It can be seen that a common mode current is generated during transients 1 and 2. During transient 3, S_5 and S_8 are opened so that the eGaN FETs conduct in the opposite direction and therefore do not generate a common mode current due to weak $\frac{\Delta v}{\Delta t}$.

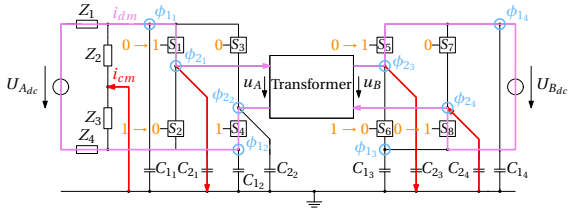

Fig. 4: Electric circuit diagram of transient 1

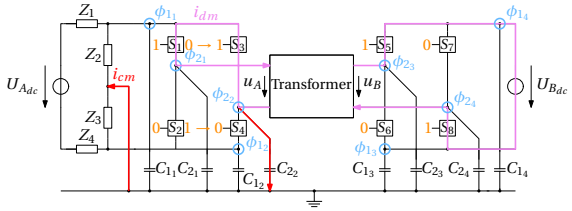

Fig. 5: Electric circuit diagram of transient 2

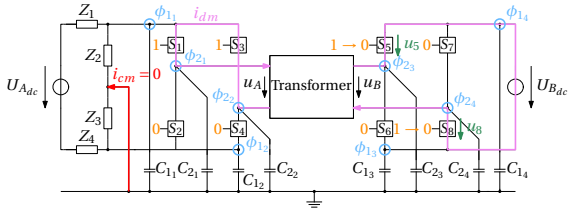

Fig. 6: Electric circuit diagram of transient 3

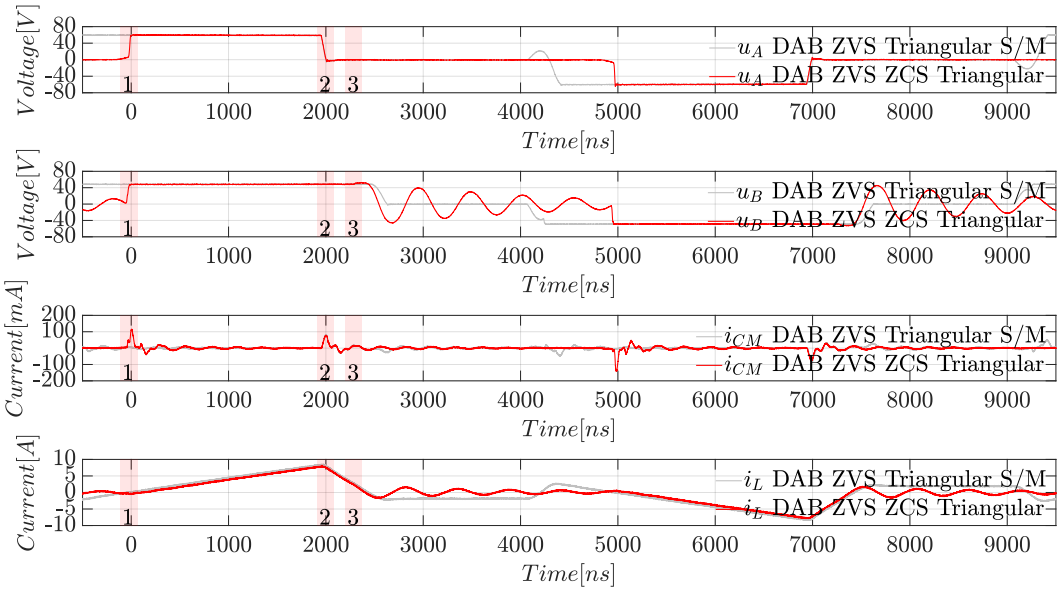

Fig. 7: DAB ZVS ZCS Triangular modulation pattern measurement results

C. DAB ZVS Triangular S/M modulation pattern common mode current evaluation in the time domain

Transient	Description
1	By switching on S_3, the potential ϕ_{2_2} increase with a positive and large $\frac{\Delta v}{\Delta t}$ and lead to a positive common mode current Figure 8.
2	By switching on S_7, the potential ϕ_{2_4} increase with a positive and large $\frac{\Delta v}{\Delta t}$ and lead to a negative common mode current Figure 9.
3	By switching on S_4 and S_6, the potentials ϕ_{2_2} and ϕ_{2_3} decrease with a negative $\frac{\Delta v}{\Delta t}$ and they do not lead to additional common mode current Figure 10.
4	By switching on S_2, the potential ϕ_{2_1} decrease with a negative and large $\frac{\Delta v}{\Delta t}$ and by switching on S_3, the potential ϕ_{2_2} increase with a positive and large $\frac{\Delta v}{\Delta t}$. This leads to a negative common mode current.

TABLE II: DAB ZVS Triangular S/M modulation pattern summary of common mode current generation

Figure 12 shows the measurement results of the DAB ZVS Triangular S/M modulation pattern. The transients that generate the common mode current are marked as blue shaded areas. The description of the respective transients can be seen in Table II. Figure 8 to Figure 11 also graphically show the switch states that generate the common mode current. It can be seen that a common mode current is generated during transients 1, 2 and 4, although the generated common mode current during transient 2 is significantly smaller than for the other transients. During transient 3, no common mode current seems to be generated.

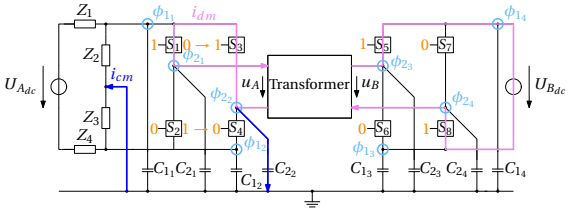

Fig. 8: Electric circuit diagram of transient 1

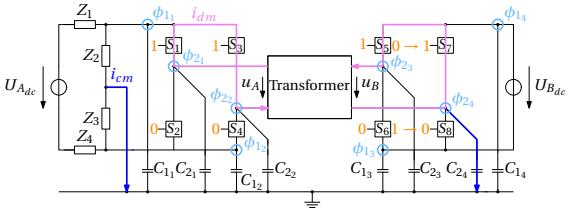

Fig. 9: Electric circuit diagram of transient 2

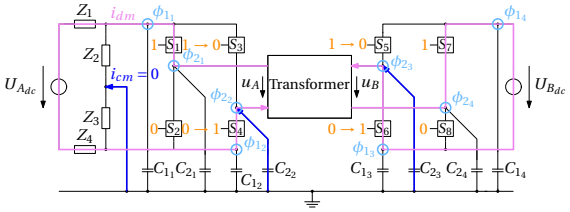

Fig. 10: Electric circuit diagram of transient 3

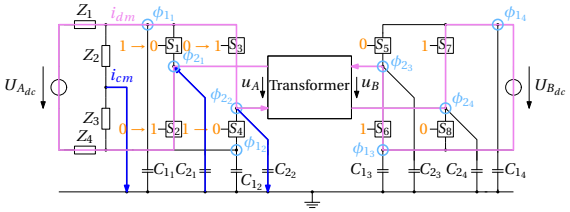

Fig. 11: Electric circuit diagram of transient 4

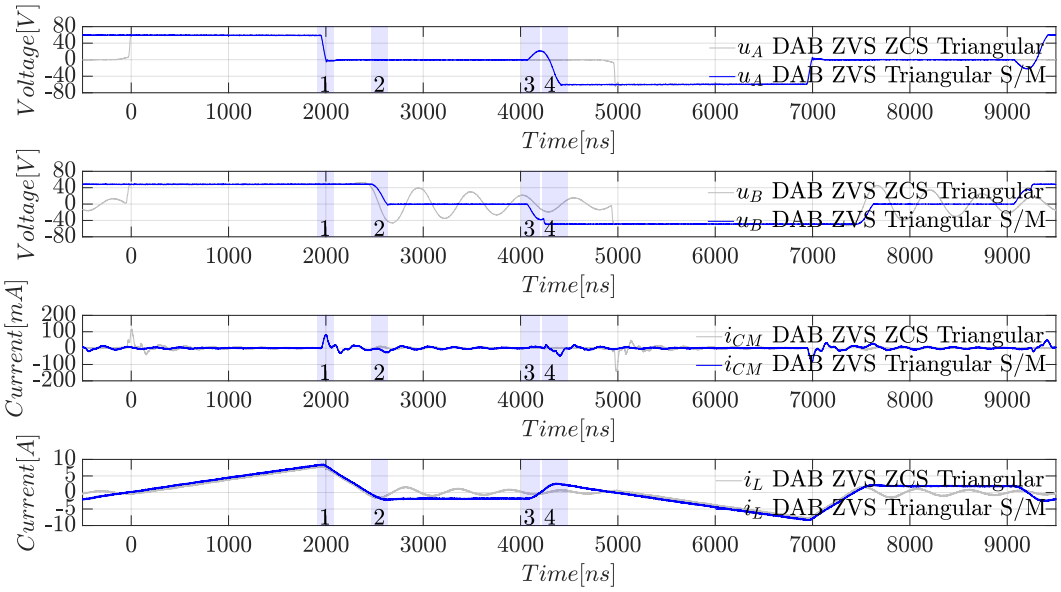

Fig. 12: DAB ZVS Triangular S/M modulation pattern measurement results

D. DAB ZVS ZCS Triangular and DAB ZVS Triangular S/M modulation patterns common mode current frequency spectrum analysis

A good way to compare the common mode current generated by DAB ZVS ZCS Triangular and DAB ZVS Triangular S/M modulation patterns is the frequency spectrum analysis. On Figure 13, the common mode current amplitude spectrum of the DAB ZVS ZCS Triangular is visible in red and of the DAB ZVS Triangular S/M modulation pattern in blue, respectively. The amplitude spectrum of the measured common mode currents was calculated and visualized using Matlab. To see the difference in the generated common mode currents, the quantity $20log_{10}(K)$ was calculated. If $20log_{10}(K) < 0\,\mathrm{dB}$, DAB ZVS Triangular S/M modulation pattern leads to a smaller common mode current and if $20log_{10}(K) > 0\,\mathrm{dB}$, DAB ZVS ZCS Triangular modulation pattern leads to a smaller common mode current. The illustration of $20log_{10}(K)$ is visible on Figure 14. The following can be interpreted from this:

- 2 kHz - 600 kHz: i_{cm} attenuated at up to $-18\,\mathrm{dB}$ with DAB ZVS Triangular S/M modulation pattern
- 600 kHz - 1.2 MHz: i_{cm} amplified at up to 10 dB with DAB ZVS Triangular S/M modulation pattern
- 1.2 MHz - 2.6 MHz: i_{cm} attenuated at up to $-10\,\mathrm{dB}$ with DAB ZVS Triangular S/M modulation pattern
- 2.6 MHz - 3.2 MHz: i_{cm} amplified at up to 10 dB with DAB ZVS Triangular S/M modulation pattern
- 3.2 MHz - 1 GHz: i_{cm} smaller with DAB ZVS Triangular S/M modulation pattern (see Figure 13)

It is evident that in the frequency range from 2 kHz to 1 GHz the DAB ZVS Triangular S/M modulation pattern appears to be advantageous in terms of common mode current generation compared to the DAB ZVS ZCS Triangular modulation pattern for a wide frequency range.

III. Conclusions

The conventional DAB ZVS ZCS Triangular modulation pattern [5] and the newly proposed DAB ZVS Triangular S/M pattern were experimentally compared in terms of common mode current generation. The latter extends the ZVS region for small to medium power ratings without having to adjust the switching frequency [3] or the transformer magnetizing inductance [4], which was the case up to now. The experimental results show that the novel modulation pattern leads to less common mode current for a wide frequency range despite more frequent switching. This is an advantage, as the losses could be reduced due to the extended ZVS region and obviously no significant increase of the common mode current has to be expected.

References

[1] R.W. De Doncker, D.M. Divan, and M.H. Kheraluwala. “A three-phase soft-switched high power density DC/DC converter for high power applications”. In: *Conference Record of the 1988 IEEE Industry Applications Society Annual Meeting*. 1988, 796–805 vol.1. DOI: 10.1109/IAS.1988.25153.

[2] F.C. Lee. “High-frequency quasi-resonant converter technologies”. In: *Proceedings of the IEEE* 76.4 (1988), pp. 377–390. DOI: 10.1109/5.4424.

[3] Dingsihao Lyu et al. “ZVS-Optimized Constant and Variable Switching Frequency Modulation Schemes for Dual Active Bridge Converters”. In: *IEEE Open Journal of Power Electronics* 4 (2023), pp. 801–816. DOI: 10.1109/OJPEL.2023.3319970.

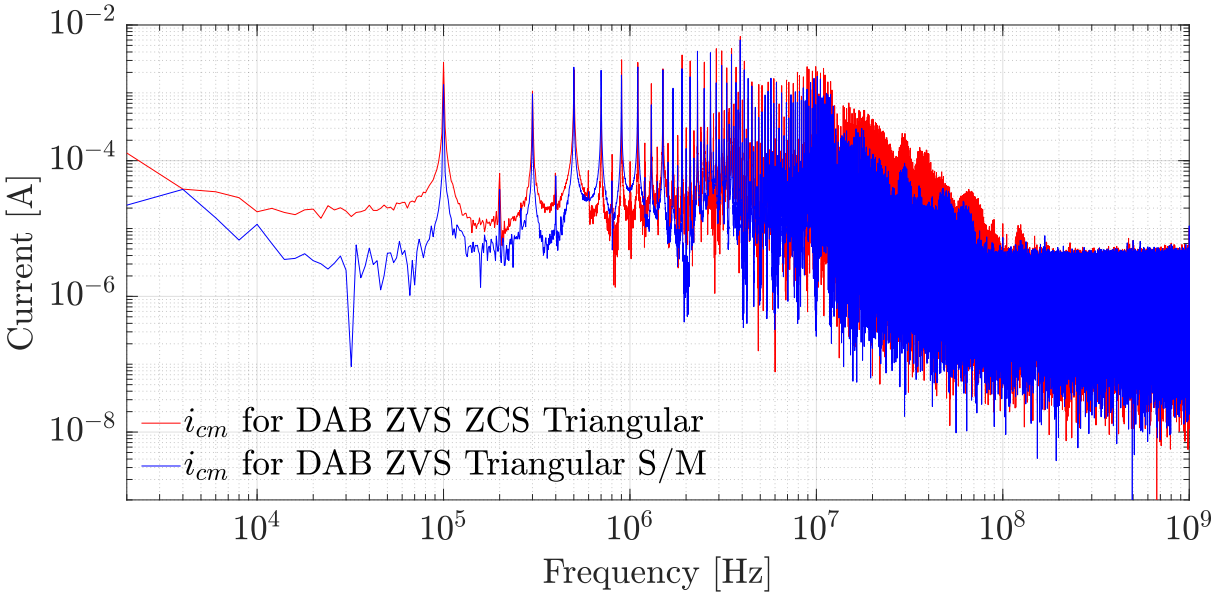

Fig. 13: Common mode current amplitude spectrum $|\mathcal{F}\{i_{cm}\}|$ of the DAB ZVS ZCS Triangular and DAB ZVS Triangular S/M modulation patterns

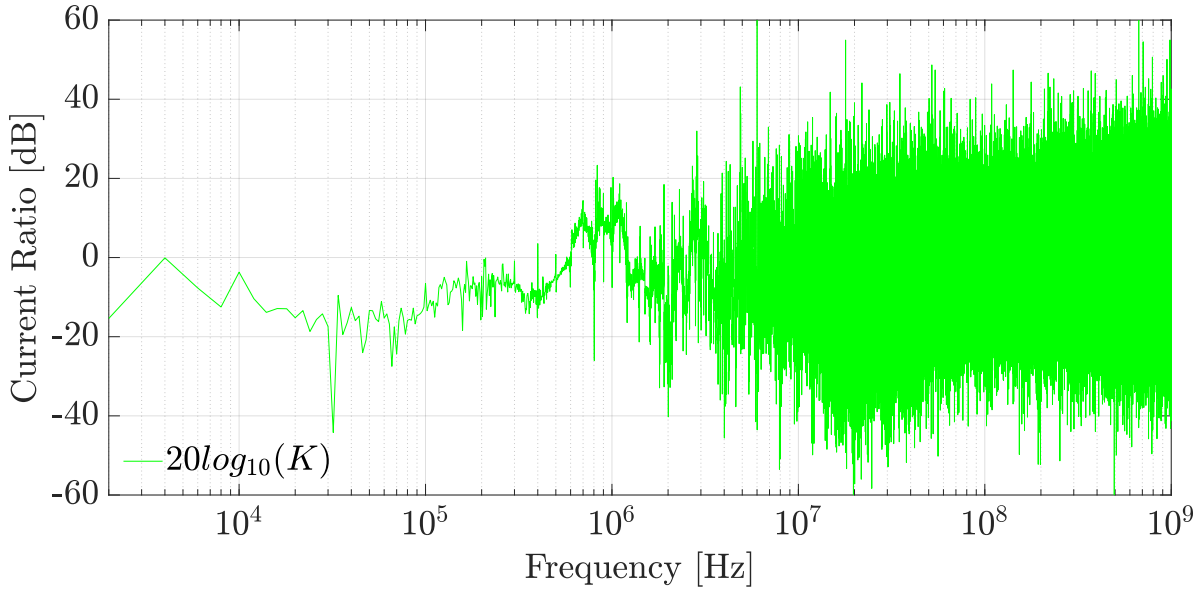

Fig. 14: Common mode current ratio $20log_{10}(K)$ with $K = \frac{|\mathcal{F}\{i_{cm}\}| \text{ of DAB ZVS Triangular S/M}}{|\mathcal{F}\{i_{cm}\}| \text{ of DAB ZVS ZCS Triangular}}$

[4] Jordi Everts et al. “Switching control strategy for full ZVS soft-switching operation of a Dual Active Bridge AC/DC converter”. In: *2012 Twenty-Seventh Annual IEEE Applied Power Electronics Conference and Exposition (APEC)*. 2012, pp. 1048–1055. DOI: 10.1109/APEC.2012.6165948.

[5] Nie Hou and Yun Wei Li. “Overview and Comparison of Modulation and Control Strategies for a Nonresonant Single-Phase Dual-Active-Bridge DC–DC Converter”. In: *IEEE Transactions on Power Electronics* 35.3 (2020), pp. 3148–3172. DOI: 10.1109/TPEL.2019.2927930.

[6] Rolf Heine Hochfrequenztechnik. “Fourline-V-LISN Type NNB-4/63TL”. rolfheine.de. Accessed: July 22, 2024. [Online]. Available: https://www.rolfheine.de/NNB463TL.html.

[7] J.C. Crebier, J. Roudet, and J.L. Schanen. “Problems using LISN in EMI characterization of power electronic converters”. In: *30th Annual IEEE Power Electronics Specialists Conference. Record. (Cat. No.99CH36321)*. Vol. 1. 1999, 307–312 vol.1. DOI: 10.1109/PESC.1999.789020.

[8] Tektronix. “P6021”. tek.com. Accessed: July 22, 2024. [Online]. Available: https://www.tek.com/de/current/p6021-manual/p6021.

[9] Tektronix. “TCPA300/400, TCP300/400 Instruction Manual”. tek.com. Accessed: July 22, 2024. [Online]. Available: https://www.tek.com/de/current/tcpa300-manual/tcpa300-400-tcp300-400-instruction-manual.

[10] Tektronix. “THDP0100/0200 & TMDP0200 Probes”. tek.com. Accessed: July 22, 2024. [Online]. Available: https://www.tek.com/de/differential-probe-manual/thdp0100-0200-tmdp0200-probes.

[11] EPC. “EPC2302 - Enhancement Mode Power Transistor”. epc-co.com. Accessed: July 22, 2024. [Online]. Available: https://epc-co.com/epc/products/gan-fets-and-ics/epc2302.